Possibility of HIV-1 protease inhibitors-clinical trial drugs as repurposed drugs for SARS-CoV-2 main protease: A Molecular docking, Molecular dynamics and Binding free energy simulation study

Iruthayaraj Ancy, Mugudeeswaran Sivanandam and Poomani Kumaradhas*
Laboratory of Biocrystallography and Computational Molecular Biology
Department of Physics, Periyar University, Salem-636 011, India

*To whom the correspondence should be addressed: Tel:+914272345857 Fax:+914272345124
E-mail: kumaradhas@yahoo.com

Abstract

Initially, the SARS-CoV-2 virus was emerged from Wuhan, China and rapidly spreading across the world and urges the scientific community to develop antiviral therapeutic agents. Among several strategies, drug repurposing will help to react immediately to overcome COVID-19 pandemic. In the present study, we have chosen two clinical trial drugs TMB607 and TMC310911 are the inhibitors of HIV-1 protease to use as the inhibitors of SARS-CoV-2 main protease (M^{pro}) enzyme. To make use of these two inhibitors as the repurposed drugs for COVID-19, it is essential to know the molecular basis of binding mechanism of these two molecules with the SARS-CoV-2 main protease (M^{pro}). Understand the binding mechanism; we performed the molecular docking, molecular dynamics (MD) simulations and binding free energy calculations against the SARS-CoV-2 M^{pro}. The docking results indicate that both molecules form intermolecular interactions with the active site amino acids of M^{pro} enzyme. However, during the MD simulations, TMB607 forms strong interactions with the key amino acids of M^{pro} and remains intact. The RMSD and RMSF values of both complexes were stable throughout the MD simulations. The MM-GBSA binding free energy values of both complexes are -43.7 and -34.9 kcal/mol, respectively. This *in silico* study proves that the TMB607 molecule binds strongly with the SARS-CoV-2 M^{pro} enzyme and it is suitable for the drug repurposing of COVID-19 and further drug designing.

Keywords: SARS-COV-2 M^{pro}; HIV-1 Protease clinical trial drugs; Drug repurposing; Molecular docking; Molecular dynamics; Binding free energy

1. Introduction

World health organization (WHO) declared global public health emergency due to the outbreak of Severe Acute Respiratory Syndrome-Coronavirus-2 (SARS-CoV-2) from the city of Wuhan, China in December 2019; subsequently, so far 192 countries were affected over the world (Minah *et al.*, 2020). Coronaviruses are the family of enveloped positive strand RNA viruses, in which SARS-CoV-2 belongs to β-coronavirus and has severe infectivity and transmissibility than SARS-CoV and MERS-CoV (Su, S.,et. al., 2016; Zhu, N., et al., 2019;

Tang, B., et al., 2020). Generally, the coronaviruses (CoV) are enveloped viruses, consist of structural proteins such as spike (S), membrane (M), envelope (E) and nucleocapsid (N) (Hossam *et al*., 2020).The S-spike protein of SARS-CoV-2 binds with the angiotensin-converting enzyme 2 (ACE2) with 10 fold more rapidly than SARS-CoV and facilitates infection (Li-Sheng *et al*., 2020). Further, the viral mRNA translates viral polyproteins and they are cleaved into functional polypeptides by SARS-CoV-2 main protease (M^{pro}),which plays an important role in the development of new viruses. Hence, targeting M^{pro} and developing the potential inhibitor will help to control the disease progression. The SARS-CoV-2 M^{pro} acts as an attractive target and the structure of viral M^{pro} contains 306 amino acids with three major domains (I-III) and 11 cleavage sites for single polyprotein1ab. The domains I and II forms a deep cleft where the substrate binding site occurs and the catalytic dyad (His41 and Cys145) present in the centre of the site (Xiaoyu *et al*., 2008;Linlin *et al*., 2020). In addition, the substrate binding site has conserved amino acids that are critical for pocket formation and they are common in all other CoVs including Leu27, Tyr53, His41, Phe139, Gly142, His163, Glu166, Leu167, His172, Asp187 and Gln192.Hence, to inhibit this viral protease, drugs should form strong interactions with these conserved amino acids and the catalytic dyad. To solve the drug crisis, the drug repurposing strategy is being adopted and it is functional in this global health emergency; the present work provides strong evidence for the drug activity and possible for drug repurposing. Currently, the anti-viral drugs lopinavir, ritinovir (HIV protease inhibition) and osletamivir (influenza virus) are being used to treat the severe infected patients of COVID-19 (https://www.the-scientist.com/news-opinion/flu-and-anti-hiv-drugs-show-efficacyagainstcoronavirus-67052). However, still hunting a potential drug from the approved/clinical trial drugs to be used as the repurposed drugs is in progress. Based on this study, we have chosen two clinical trial drugs (inhibitors) of HIV-1 protease (Scheme 1) (i) un-boosted TMB607 (suspended at phase I clinical trial for new study site selection during April

2019) (https://clinicaltrials.gov/ct2/show/NCT03110549) and (ii) TMC310911 boosted with ritonavir (completed phase IIa clinical trial) (https://clinicaltrials.gov/ct2/show/NCT00838162) shown in Figure 1.The drugs were found to be safe and well tolerated among the healthy volunteers with no-dose limiting toxicity (Stellbrink, *et al*., 2014; Jinzi *et al*., 2006). The molecular binding mechanism of these two drugs in the active site of SARS-CoV-2 M^{pro} enzyme is not yet known; to understand the same, we have carried out the molecular docking, molecular dynamics (MD) simulations and binding free energy calculations. The detailed information about the stability of the drug molecules in the active site of SARS-CoV-2 M^{pro} enzyme, intermolecular interactions with the amino acids of binding site and their binding affinity are provided here from the molecular docking and MD simulations. These results are useful to evaluate these two clinical trial drugs to consider as the repurposed drugs to treat the devastated COVID-19 disease after *in vitro* and clinical studies.

2. Materials and Methods

2.1 Ligand preparation and Molecular docking

The geometry of molecules TMC310911 and TMB607 were optimized with B3LYP/6-311G** level of density functional theory (DFT) (Davidson & Feller, 1986; Parr & Yang, 1989) using *Gaussian03* software (Frisch et al., 2005). Selected two molecules were prepared by optimized potentials for liquid simulations (OPLS_2005). The X-ray crystal structure of SARS-CoV-2 M^{pro} (PDB: 6LU7) was retrieved from Protein Data Bank (PDB). The structure was optimized with OPLS_2005 force field using protein preparation wizard of *Maestro* application incorporated in the *Schrödinger programme* suit LLC (Jacobson et al., 2004). Induced fit docking (IFD) was carried out for these two compounds with SARS-CoV-2 M^{pro}. In the IFD, the standard protocol was chosen; gird box was centred on the catalytic site residues. The van der Waals scaling of both protein and ligands were fixed at 0.50. Finally, *extra precision* (XP) mode of IFD was performed. The intermolecular interactions and electrostatic potential map of both ligand-M^{pro}

complexes were analyzed using *PyMol* (DeLano, 2002) and *Discovery studio visualizer* software (Dassault Systems BIOVIA 2017).

2.2 MD simulation and Binding free energy calculations

The MD simulations of TMC310911-SARS-CoV-2 M^{pro} and TMB607-SARS-CoV-2 M^{pro} complexes were carried out using *Sander* routine of *AMBERTOOLS14* package (Case et al., 2014) to understand the stability and the binding nature of the two molecules in the substrate binding site of SARS-CoV-2 M^{pro} enzyme. The orthorhombic shell of TIP3P water box were generated with a minimum solute-wall at 8 Å distance and to neutralize the charges of the complex system4 Na^+ ions were added for the removal of steric clashes present in the complexes. Further, both complexes were minimized and annealed from 0 to 300 K for 500ps time period and equilibrated at 300 K for 500pswith the maintenance of canonical ensemble (NVT) (Glenn J.M. et al., 1999).The MD production phase was initiated and continued to 50ns in 2fs time step at constant temperature (300 K) and pressure (1 bar) using Langevin thermostat and Berendsen barostat as in the heating process (Andrew & Ben 2011; Berendsen, et al., 1984). *VMD* (Humphrey, et al., 1996) and *CPPTRAJ* software (Daniel & Cheatham 2013) were used to analyze the MD trajectory. MM-GBSA calculation was carried out for both complexes based on GB model (Onufriev et al., 2000).

3. Results and discussion

3.1 Molecular docking and Intermolecular interactions

The glide energy of TMB607-SARS-CoV-2 M^{pro} and TMC310911-SARS-CoV-2 M^{pro} complexes were obtained from the molecular docking simulation, the values are -10.3 and -7.1 kcal/mol, respectively. The intermolecular interactions of TMB607 and TMC310911 molecules with the SARS-CoV-2 M^{pro} enzyme were identified and presented in Table 1 & 2. The H27 atom of molecule TMB607 forms hydrogen bonding interactions with one of the catalytic dyad amino acids Cys145 with the distance 3.0 Å. In addition, the molecule also forms π···π stacked type of hydrophobic interaction with the amino acid His41 at the distance 4.2 Å. And

TMB607also forms hydrogen bonding interaction with Glu166 at the distance 3.4 Å and alkyl···π-orbital type of hydrophobic interaction with His163 at the distance 4.8 Å, which isone of the conserved amino acids of M^{pro} enzyme. In contrast to TMB607, the molecule TMC310911 only forms alkyl···π-orbital type of interaction with the catalytic dyad amino acid His41 at the distance 4.9 Å and hydrogen bonding interaction with the conserved amino acids Glu166 and Leu167 at the distance 2.7 and 2.3 Å, respectively (Fenghua et al., 2016). Further, to understand the conformation, stability, intermolecular interactions and binding affinity of both drug molecules with the M^{pro}, MD simulation has been carried out.

3.2 Evaluation of MD simulation and Intermolecular interactions

The MD simulations for the TMB607-SARS-CoV-2 M^{pro} and TMC310911-SARS-CoV-2 M^{pro} complexes have been carried out for 50ns. Figure 2 shows the RMSD and RMSF values of both complexes and are found to be stable over the 50ns simulations; in which notably, the RMSD values of the TMB607-SARS-CoV-2 M^{pro} complex are less (~1.5 Å) than the TMC310911-SARS-CoV-2 M^{pro} complex (~3.5 Å) over the entire simulations, confirms the high stability of TMB607-SARS-CoV-2 M^{pro} complex. Further, the RMSF values illustrate that, the fluctuations of active site residues are found to be low for both complexes, however the RMSF values of TMB607-SARS-CoV-2 complex is lower than TMC310911-SARS-CoV-2 M^{pro} complex. This difference reveals the strong interactions between TMB607 and the active site residues of SARS-CoV-2-M^{pro}.

The intermolecular interactions between each drug molecule with the neighbouring amino acids present in the active site of SARS-CoV-2 M^{pro} of TMB607-SARS-CoV-2 M^{pro} and TMC310911-SARS-CoV-2 M^{pro} complexes observed during the MD simulation are listed in Table 1 & 2 respectively. The hydrogen bonding interactions of the complex is shown in Figure 3. It is found that at the 50ns MD simulation, the molecule forms strong interactions with the amino acids His41 and Cys145 of catalytic dyad, which is stronger than the same found in

docked complex and the corresponding hydrogen bonding interaction distances are 2.8 and 2.5 Å, respectively. Further, the molecule also forms strong hydrogen bonding interaction with the conserved amino acids including Glu166, Gln189 and Gln192 at the distance 2.7, 1.9, 1.9 Å, respectively and alkyl···π-orbital type of hydrophobic interaction with the residue His163 at the distance of 4.8 Å, respectively. Figure 4 shows the strong intermolecular interactions of TMC310911-SARS-CoV-2 M^{pro} complex. Here, at the 50ns of MD simulation, the molecule almost lost all interactions with the conserved amino acids except Glu166 with the distance of 2.0 Å. This indicates that the molecule almost shifted from the substrate binding site during the MD simulation, confirms that the molecule is less stable in the active site and the representation Connolly surface plots of ligand binding of both molecules displays the position of the ligands in the active site (Figure 5).

3.3 Binding free energy

The MM-GBSA, MM-PBSA and decomposition free energy values of TMB607-SARS-CoV-2 M^{pro} and TMC310911-SARS-CoV-2 M^{pro} complexes were calculated from the MD trajectories. The MM-GBSA free energy values of both complexes are -43.7 and -34.9 kcal/mol, respectively. Contributions of various energy components to the binding free energy for TMB607 and TMC310911 with SARS-CoV-2 M^{pro} of both complexes are listed in Table 3. The decomposition free energy values of these two complexes are plotted in Figure 6. In concurrence with the intermolecular interaction results, the TMB607 molecule contributes low decomposition free energy with the catalytic dyad amino acids His41 (-1.4 kcal/mol) and Cys145 (-1.9 kcal/mol) and conserved residues including Leu167 (-1.3 kcal/mol), Gln189 (-4.4 kcal/mol) and Gln192 (-1.6 kcal/mol), respectively. The decomposition free energy contribution of the molecule TMC310911 with the conserved residues is quite higher than TMB607. The molecule has low binding energy contribution with the conserved amino acids Leu167 (-1.9 kcal/mol) and Gln189 (-0.97 kcal/mol).

4. Conclusion

HIV-1 protease inhibitor combinations are being used to treat severe infected COVID-19 patients successfully. The search of drugs from the approved/clinical trial drugs to be used as the repurposed drugs is in progress everywhere. In the present study, we have chosen two clinical trial HIV-1 protease inhibitors TMB607 and TMC310911 and performed molecular docking, MD simulation and binding free energy calculations. The docking analysis shows the glide energy value of the molecule TMB607 (-10.3 kcal/mol) is lower than TMC310911 (-7.1 kcal/mol). The molecule TMB607 forms strong interactions with the catalytic dyad residues His41 and Cys145. Further, the RMSD and RMSF values of both complexes were remain stable during the MD simulations. However, the RMSD and RMSF values of TMB607-SARS-CoV-2-M^{pro} complex are found to be low on compare withTMC310911. During the MD simulation, the molecule TMB607 forms strong intermolecular interactions with the catalytic dyad residues His41 and cys145 and the conserved residues including Glu166, Gln189 and Gln192. Notably, the molecule forms strong interaction with the NH of His41 and SG of Cys145. Further, the SG of Cys145 is nucleophillic in nature, and plays a crucial role in proteolytic process (Tanigaimalai *et al*., 2016). Whereas, the molecule TMC310911 form strong interaction with the conserved residue Glu166 alone. These interactions are in correlation with the recently reported inhibitor α-ketomide (Linlin *et al*., 2020). The MM-GBSA and decomposition free energy values also confirm the high potency of the molecule TMB607 against SARS CoV-2 M^{pro}. Hence, from the present study, we suggest that the molecule TMB607 is standalone and unboosted (with ritinovir) drug shall be the promising highly stable candidate to inhibit the SARS-CoV-2 M^{pro} and can be used as a repurposed drug to treat the devastating COVID-19 virus disease and further drug designing.

Acknowledgements

The authors thank the Computer Centre, Periyar University, Salem to perform the computational work in the High Performance Cluster (HPC) Computer.

References

Andrew, J., & Ben, L. (2011). Adaptive stochastic methods for sampling driven molecular systems, *Journal of Chemical Physics.*135, 084125. doi: 10.1063/1.3626941.

Berendsen, H. J. C., Postma, J. P. M., van Gunsteren, W. F., Di Nola, A., &Haak, J. R. (1984).Molecular dynamics with coupling to an external bath.*Journal of Chemical Physics.* 81, 3684-3690. doi:10.1063/1.448118.

Case, D. A., Babin, V., Berryman, J. T., Betz, R. M., Cai, Q., Cerutti, D. S., Cheatham, T. E., Darden, T. A., Duke, R. E., Gohlke, H., Goetz, A. W., Gusarov, S., Homeyer, N., Janowski, P., Kaus, J., Kolossváry, I., Kovalenko, A., Lee, T. S., Le Grand, S., Luchko, T., Luo, R.,Madej, B., Merz, K. M.,Paesani, F., Roe, D. R.,Roitberg, A.,Sagui, C., Salomon-Ferrer, R.,Seabra, G., Simmerling, G. L., Smith, W.,Swails, J., Walker, R. C., Wang, J., Wolf, R. M., Wu, X., and Kollman, P. A., (2014), *AMBER 14*, University of California, San Francisco.

Daniel R.R., & Cheatham, T. E. (2013). PTRAJ and CPPTRAJ: Software for Processing and Analysis of Molecular Dynamics *Trajectory Data. Journal of Chemical Theory and Computation,* 9, 3084-3095. doi:10.1021/ct400341p doi: 10.1021/ct400341p

Dassault Systems BIOVIA.(2017). Discovery studio modeling environment, release. San Diego, CA: Author.

Delano, W. L. (2002). PyMol molecular graphics system. San Carlos, CA: Delano Scientific.

Fenghua, W., Cheng, C, Wenjie, T., Kailin, Y &Haitao, Y (2016).Structure of Main Protease from Human Coronavirus NL63:Insights for Wide Spectrum Anti-Coronavirus Drug Design. *Scientific Reports,* 6, 22677;doi: 10.1038/srep22677.

Frisch, M. J., Trucks, G. W., Schlegel, H. B., Scuseria, G. E., Robb, M. A., Cheeseman, J. R., … Pople, J.A. (2004). Wallingford, CT: *Gaussian*.

Glenn, J. M., Adam, H.& Tuckerman, M. E. (1999).Molecular dynamics algorithms for path integrals at constant pressure. *Journal of chemical physics*. 110, 3275-3290. doi: 10.1063/1.478193

https://clinicaltrials.gov/ct2/show/NCT00838162.

https://clinicaltrials.gov/ct2/show/NCT03110549.

https://www.the-scientist.com/news-opinion/flu-and-anti-hiv-drugs-show-efficacy againstcoronavirus-67052.

Humphrey, W., Dalke, A. &Schulten, K. (1996).VMD-Visual Molecular Dynamics.*Journal of Molecular Graphics. 14*, 33-38.doi: 10.1016/0263-7855(96)00018-5

Hossam M. A, Walid F. EMd. Masudur R and Hatem A. E (2020).Insights into the Recent 2019 Novel Coronavirus (SARS-CoV-2) in Light of Past Human Coronavirus Outbreaks Pathogens, 9, 186, 1-15 doi: 10.3390/pathogens9030186

Jacobson, M. P., Pincus, D. L., Rapp, C. S., Day, T. J. F., Honig, B., Shaw, D. E. &Friesner, R. A. (2004) "A Hierarchical Approach to All-Atom Protein Loop Prediction, Proteins: *Structure, Function and Bioinformatics*, 55, 351-367.doi: 10.1002/prot.10613

Jinzi J. Wu B. R. S., Milot G., Ge M., Dandache S., Forte A., Pelletier I., Dubois A., Belanger O. &Panchal C. (2006). Pl-100, a next generation protease inhibitor against drug-resistant HIV: In vitro & in vivo metabolism. *46th Annual ICAAC Interscience Conference on Antimicrobial Agents and Chemotherapy Sept 27-30, 2006, San Francosco.*

Labanowski, J. K., &Andzelm, J. W. (1991).Density functional methods in chemistry. New York, NY: Springer.

Linlin Z., Daizong, L., Xinyuanyuan, S., Ute, C., Christian D., Lucie, S., Stephan, B., Katharina R. & Rolf H. (2020).Crystal structure of SARS-CoV-2 main protease provides abasis for design of improved α-ketoamide inhibitors. *Science* (In press) doi: 10.1126/science.abb3405.

Li-sheng, W., Yi-ru, W., Da-wei, Y., &Qing-quan, L. (2020). A review of the 2019 Novel Coronavirus (COVID-19) based on current evidence. *International Journal of Antimicrobial Agents*.doi:10.1016/j.ijantimicag.2020.105948.

Minah, P., Alex, R. C., Jue T. L., Yinxiaohe S. &Borame L. D (2020) A Systematic Review of COVID-19 Epidemiology Based on Current Evidence. *Journal of clinical medicine, 9*, 967.doi:10.3390/jcm9040967.

Onufriev, A., Bashford, D. & Case, D.A, (2000). Modification of the Generalized Born Model Suitable for Macromolecules, *Journal of Physical Chemistry B, 104*, 3712–3720.doi: 10.1021/jp994072s.

Parr, R. G., & Yang, W. Density functional theory of atoms and molecules. (1989). New York, NY: Oxford.

Su, S., Wong ,G., Shi, W., Liu, J., Lai, A.C.K., Zhou, J., Liu,W., Bi, Y. & Gao, G, F. (2016). Epidemiology, Genetic Recombination, and Pathogenesis of Coronaviruses. *Trends in Microbiology, 24(6), 490-502.* doi: 10.1016/j.tim.2016.03.003

Stellbrink, H. J., Arasteh, K., Schürmann, D., Stephan, C., Dierynck, I., Smyej, I., Hoetelmans, R. M. W., Truyers, C., Meyvisch, P., Jacquemyn, B., Mariën, K., Simmen, K. &Verloes, R(2014). Antiviral Activity, Pharmacokinetics, and Safety of the HIV-1 Protease Inhibitor TMC310911, Co administered With Ritonavir, in Treatment-Naive HIV-1–Infected Patients (2014). *Journal of Acquired Immuno Deficiency Syndrome* 65(3), 283-289. doi: 10.1097/QAI.0000000000000003

Tang, B., Bragazzi, N.L., Li, Q., Tang, S., Xiao, Y. & Wu, J. (2020). An updated estimation of the risk of transmission of the novel coronavirus (2019-nCov). *Infect Dis Model. 5, 248-255*. doi: 10.1016/j.idm.2020.02.001.

Thanigaimalai, P.,Manoj, M.,Vigneshwaran, N.,Yoshio H. & Sang-Hun J. (2016). An Overview of Severe Acute Respiratory Syndrome−Coronavirus (SARS-CoV) 3CL Protease Inhibitors: Peptidomimetics and Small Molecule Chemotherapy. *Journal of Medicinal Chemistry*, 59, 6595-6628. doi: 10.1021/acs.jmedchem.5b01461

Xiaoyu, X., Hongwei, Y., Haitao, Y., Fei, X., Zhixin, W., Wei, S., Jun, Li., Zhe, Zhou., Yi, D., Qi, Z., Xuejun, C. Z., Ming, L.,Mark, B., &Zihe, R. (2008). Structures of Two Coronavirus Main Proteases: Implications for Substrate Binding and Antiviral Drug Design. *Journal of Virology*, 82(5), 2515–2527.doi: 10.1128/JVI.02114-07

Zhu, N., Zhang,D ., Wang, W., Li, X., Yang, B., Song, J., et al. (2019). A Novel Coronavirus from Patients with Pneumonia in China, 2019. *New England Journal of Medicine. 382:727-733*. doi: 10.1056/NEJMoa2001017

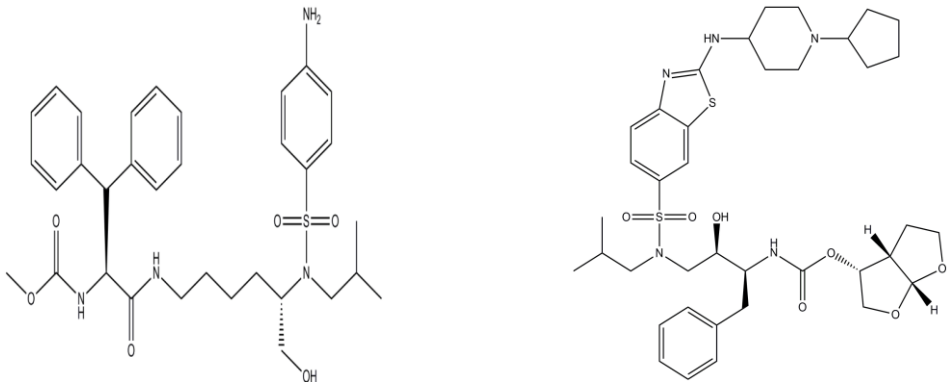

(a) (b)

Scheme 1: Chemical structure of (a) TMB607 and (b) TMC310911 molecules.

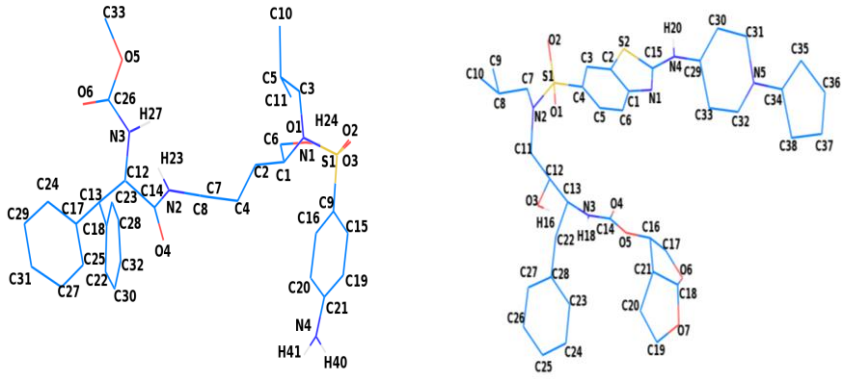

(a) (b)

Figure 1: Molecular structure and the atom labelling of (a) TMB607 and (b) TMC310911.

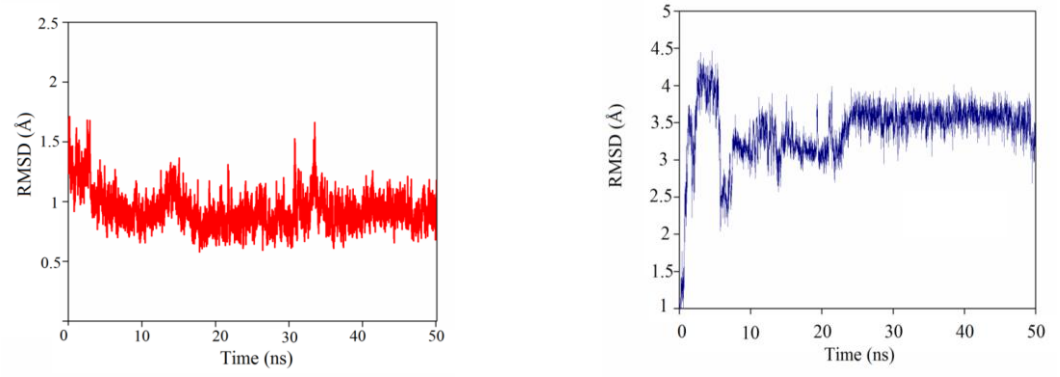

(a) (b)

Figure 2: RMSD plots of (a) TMB607 and (b) TMC310911-SARS-CoV-2 M^{pro} complexes.

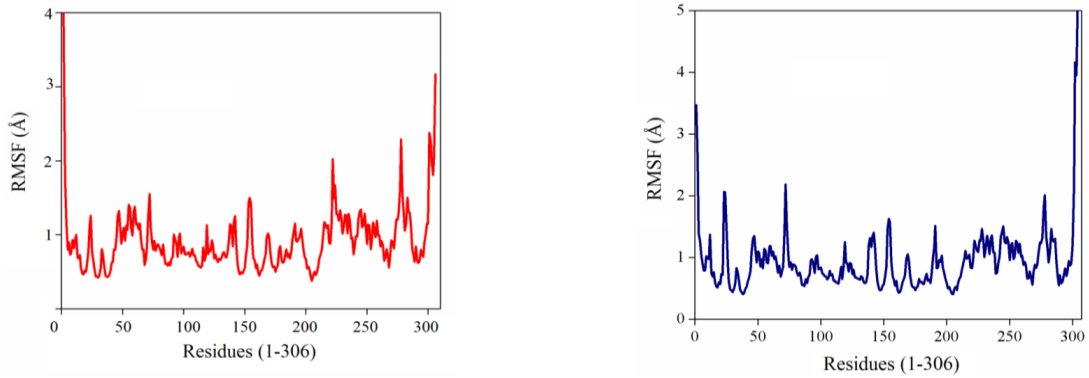

(a) (b)

Figure 3: RMSF plots of (a) TMB607 and (b) TMC310911-SARS-CoV-2 M^{pro} complexes.

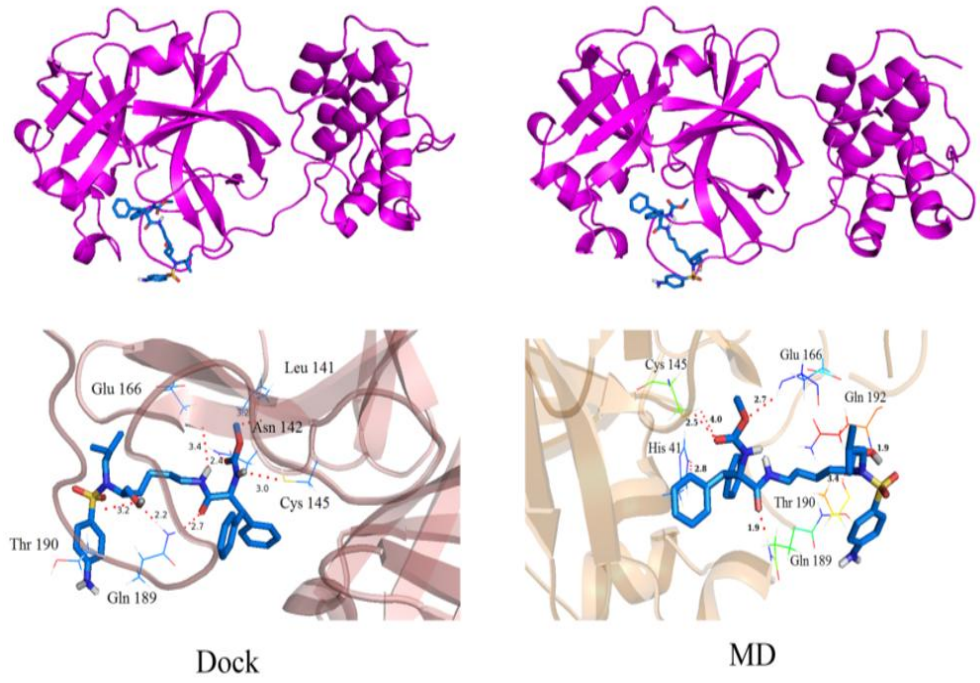

(a)

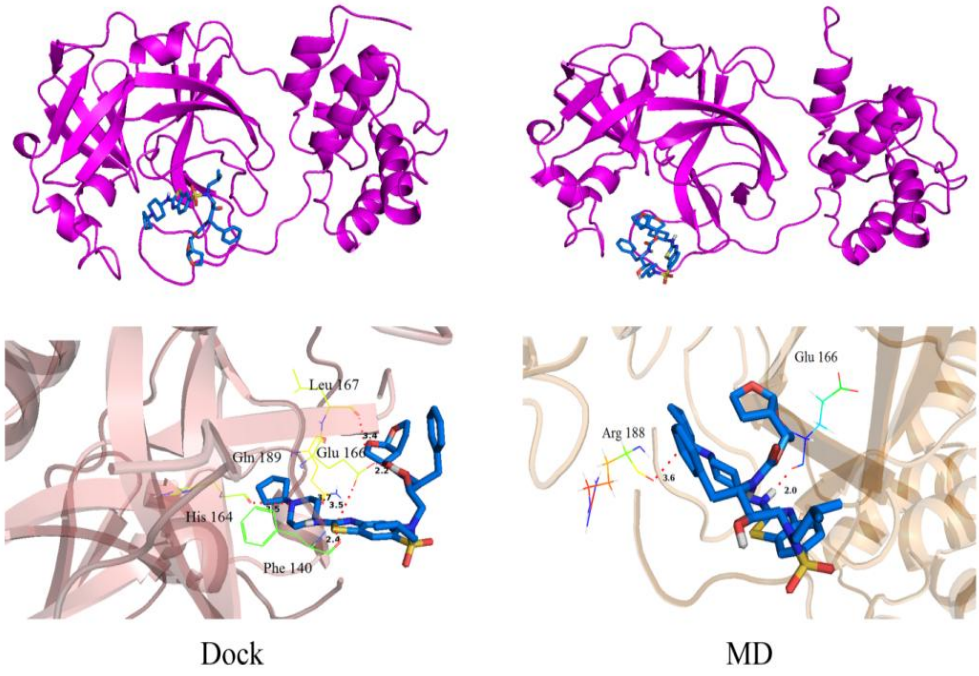

(b)

Figure 4: Intermolecular interactions of (a) TMB607-SARS-CoV-2 M^{pro} and (b) TMC310911-SARS-CoV-2 M^{pro} complexes obtained from docking and the MD simulations.

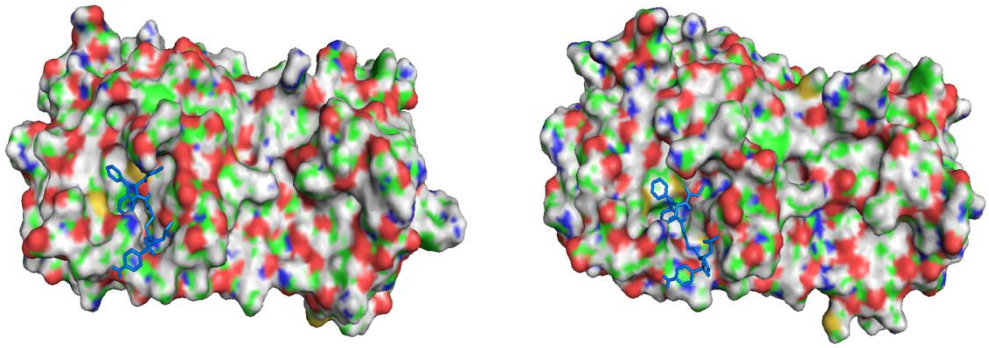

(a)

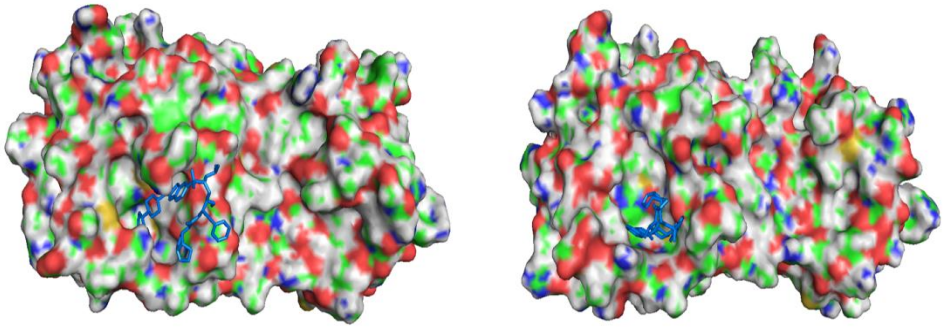

(b)

Figure 5: Connolly representation of (a) TMB607-SARS-CoV-2 M^{pro} and (b) TMC310911-SARS-CoV-2 M^{pro} complexes obtained from docking (left) and MD simulations (right).

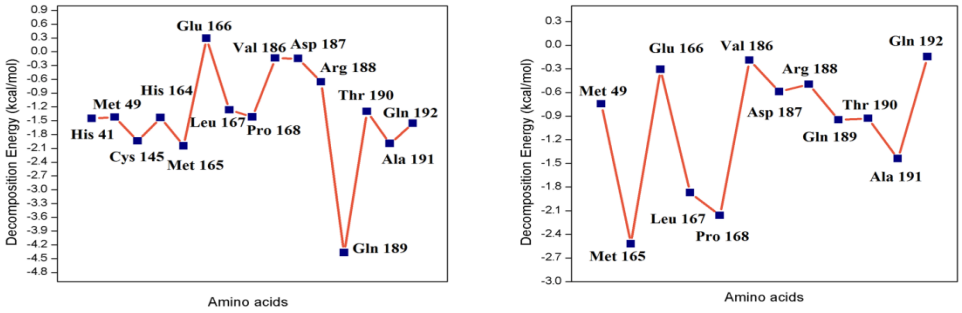

(a) (b)

Figure 6: Decomposition free energy plots of (a) TMB607-SARS-CoV-2 M^{pro} and (b) TMC310911-SARS-CoV-2 M^{pro} complexes during the MD simulations.

Table 1: Intermolecular interaction distances of TMB607···SARS-CoV-2 M^{pro} complex.

TMB607··· SARS-CoV-2 M^{pro}	Distance (Å)	
	Dock	MD
Hydrogen bonding interactions		
C33···O/Leu141	3.2	-
O6···HD21/HA/Asn142	2.4, 2.6	-
H27···SG/Cys145	3.0	-

H23···HN/Glu166	3.4	-
O5···HN/Glu166	-	2.7
O1···HE21/Gln189	2.1	-
O4···HE22/Gln189	2.7	1.9
H24, C6···O/Thr190	2.5, -	-, 3.4
O1···HNGln192	-	1.9
Hydrophobic interactions		
Lig···His41 (π-π-stacked)	4.2	-
Lig···SD/Met49 (π-orbital···Sulfur)	4.9	5.3
Lig···SG/Cys145(π-orbital···Sulfur)	5.0	5.3
Lig···His163 (alkyl···π-orbital)	4.8	4.8
Lig···His172 (alkyl···π-orbital)	5.1	-

Table 2: Intermolecular interaction distances of TMC310911···SARS-CoV-2 M^{pro} complex.

TMC310911···SARS-CoV-2 M^{pro}	Distance (Å)	
	Dock	MD
Hydrogen bonding interactions		
S2···O/Phe140	2.4	-
H40···O/His164	3.5	-
H15···OE1/Glu166	2.2	-
H20···OGlu166	-	2.0
H21···OGlu166	-	2.5
S···OE2/Glu166	3.5	-
C17···O/Leu167	3.4	-
H45···OArg188	--	2.7
C32···OE1/Gln189	3.7	-
Electrostatic interaction		
Lig···OE2/Glu166 (Anion···π-orbital)	3.6	-
Hydrophobic interactions		
Lig···His41 (π-alkyl···π-orbital)	4.9	-
Lig···Met49	-	5.0
Lig···Met165 (alkyl···alkyl)	4.7	5.5
Lig···Pro168 (alkyl···alkyl)	4.3	4.2

Table 3: Contributions of various energy components to the binding free energy (kcal/mol) for TMB607-SARS-CoV-2 $M^{pro}$and TMC310911-SARS-CoV-2 M^{pro}complexes.

Energy Components	TMB607	TMC310911
ΔE_{vdw}	-60.4	-46.6
$\Delta E_{electrostatic}$	-31.1	-12.1
$\Delta G_{PB/GB}$	51.8	-28.9
ΔE_{SA}	-7.7	-5.1
ΔE_{gas}	-87.8	-58.7
ΔG_{sol}	44.1	23.8
ΔG_{Total}	-43.7	-34.9